Astrophysics from Antarctica
Proceedings IAU Symposium No. 288, 2012
M. G. Burton, X. Cui & N. F. H. Tothill, eds.

doi:10.1017/S1743921312016791

The Exploration of the ISM from Antarctica

Mark G. Wolfire

Astronomy Department
University of Maryland
College Park, MD 20742
email: mwolfire@astro.umd.edu

Abstract. Antarctica presents a unique environment for the exploration of the interstellar medium. The low column of water vapor opens windows for sub-mm and THz astronomy from ground and sub-orbital observatories while the stable atmosphere holds promise for THz interferometry. Various current and potentially future facilities occupy a niche not available to current space or stratospheric instruments. These allow line and continuum observations addressing key questions in e.g., star formation, galactic evolution, and the life-cycle of interstellar clouds. This review presents scientific questions that can be addressed by the suite of current and future Antarctic observatories.

Keywords. ISM: general, ISM: molecules, infrared: ISM

1. Introduction

One of the great advantages of observing from Antarctica is that it is so dry. This is extremely important for sub-mm and THz observations. At Dome A, good conditions can reach $\sim 25\%$ transmission for the [C II] fine-structure transition at 158 μm and $\sim 80\%$ at the [C I] fine-structure transition at 310 μm (Lawrence 2004). High altitude balloon flights over Antarctica from McMurdo Station can see essentially the entire THz submillimeter range with little intervening opacity. Many diagnostic emission lines from a range of interstellar medium environments are accessible in the observing windows opened up by the dry conditions. For example, there are [O I], [C II], and [C I] fine-structure lines. These are collisionally excited in warm neutral gas and come from photodissociation regions or "PDRs". There are also high-J rotational transitions (e.g., CO 7-6, CO 13-12, CO 29-28) that also arise in PDRs and in shocks. There are ionized gas lines, such as [N II] that comes from compact and diffuse H II regions. Light hydrides (e.g., H_3O^+, SH) might be seen in emission or absorption and come from PDRs, and there is also the dust continuum emission.

What science questions can be addressed with observations from Antarctica? For example:

- What is the energy budget of the Galactic interstellar medium (ISM) gas as a function of position and scale height? How does radiative heating compare to turbulent heating?

- What is the distribution of "phases" and thermal pressure in the ISM. How do these compare to global models of star formation and the ISM.

- What is the distribution and physical properties of ionized gas in the Galaxy?

- What is the carbon budget? Where is carbon mainly C^+, C and CO?

• What is the life-cycle of clouds from formation to photoevaporation?

• What are the physical conditions (density and temperature) and far-ultraviolet radiation fields across giant molecular clouds (GMCs) ?

• What is the distribution and mass of "dark molecular gas" in the Galaxy and LMC/SMC?

• What are the important channels for production of molecules in diffuse gas?

A common requirement running through these sample science projects is good atmospheric transmission in the THz and sub-mm bands. Several require large scale survey mapping which can best be done from Antarctica.

2. Photodissociation Regions

Many of the THz and sub-mm emission lines arise in PDRs and we next consider in more detail the structure of PDRs. A working definition is that a photodissociation region is a gas phase in which far-ultraviolet (FUV; 6 eV $\leqslant h\nu \leqslant$ 13.6 eV) radiation plays a role in the heating or chemistry. This range of energies is responsible for dissociating molecules and also dominates the heating process. PDRs are hydrogen neutral regions and lie outside of H II regions. Historically, the radiation field has been measured in units of the integrated FUV interstellar radiation field. G_0 has become a standard notation for a Habing interstellar field and χ generally indicates a Draine field and they differ by a factor 1.7. Fields that are typically encountered range from $G_0 = 1$ for the ISRF to $G_0 = 10^5$ for the Orion Trapezium PDR.

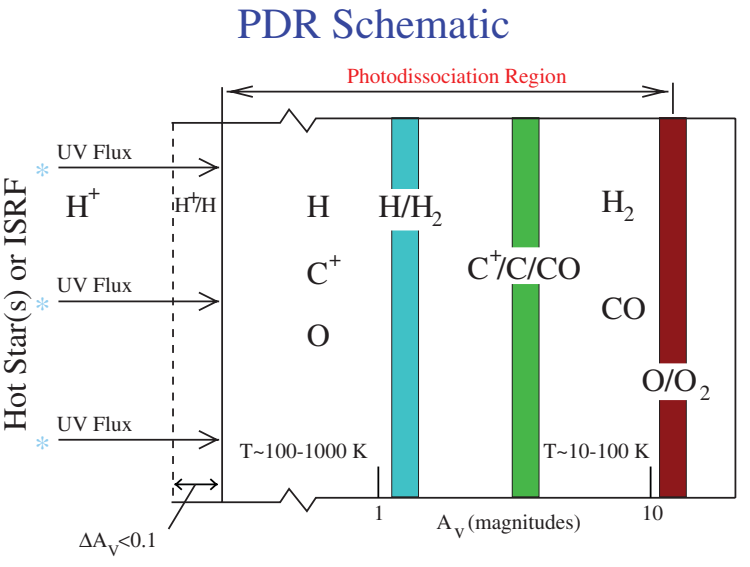

Figure 1. Schematic of PDR as a function of A_V into a cloud. Note that the peak O_2 abundance is now known to occur closer to the cloud surface (Hollenbach *et al.* 2009).

PDRs are found where OB stars shine on molecular clouds. The FUV that escapes the H II region produces a PDR on the cloud surface that can extend to an $A_V \sim 8$ though the gas. The mean column density of Galactic molecular clouds is also $A_V \sim 8$ and thus

https://doi.org/10.1017/S1743921312016791 Published online by Cambridge University Press

much of the mass in molecular gas is in PDRs. Another place PDRs are found is in the diffuse medium. The same PDR physics that works in the molecular cloud surfaces is also at work in diffuse clouds but with generally lower FUV field and lower column densities.

In addition, PDRs may contribute to emission in protostellar outflows. van Kempen *et al.* (2010) suggest that PDRs can contribute to the high-J CO emission in the protostellar walls of HH46. Gorti & Hollenbach (2009) find that in the outer parts of protostellar disks, PDRs can contribute to the heating, chemistry, and structure.

A schematic of a PDR as a function A_V is shown in Figure 1. In the outer portions of the cloud the gas is mainly neutral atomic hydrogen, helium and oxygen, and single ionization states of metals (e.g., C^+, Si^+, Mg^+, Fe^+). The dominant heating process is photoelectric heating from grains. Most of the FUV photon energy is absorbed by grains and radiated as IR continuum. As much as $\sim 5\%$ of the photon energy can be converted to gas heating via the grain photoelectric effect. The heating is balanced by [C II] 158 μm, and [O I] (63 μm, 145 μm) fine-structure line emission which can be observed from Antarctica. The balance between heating and cooling typically gives temperatures between 100 and 1000 K, but both higher and lower temperatures are possible.

Deeper into the cloud H_2 starts to form on grain surfaces and C^+ recombines to neutral carbon. The depth of the transition from the cloud surface depends on the ratio of G_0/n (Wolfire *et al.* 2010). Photoelectric heating dominates balanced by [C II], [O I], and [C I] (610 μm, 370 μm) line cooling. Additional diagnostics include the rotational and vibrational excitation of molecular hydrogen. We have also have light hydrides forming, many observable from Antarctica including H_3O^+, and SH (Gerin *et al.* 2010, Neufeld *et al.* 2012).

After C^+ recombines to C, CO starts to form and high-J CO line emission is produced followed by low-J CO line emission. Deep into the cloud the heating could be photoelectric heating, but can also be dominated by cosmic rays or coupling with warm dust. The cooling is from molecules with typical temperatures between 10 and 100 K. We next consider a few of the scientific questions that were raised in the introduction.

3. Galactic ISM Energy Budget

COBE FIRAS found a total [C II] all sky luminosity of $10^{7.7}$ $L_\odot$ (Wright *et al.* 1991), a luminosity that is ~ 4 times brighter than the combined [N II] (122 μm, 205 μm) lines and ~ 100 times brighter than the [C I] (370 μm, 610 μm) lines. We still do not know entirely which phase produces the [C II] emission which is important to know how to apportion the luminosity among the various gas phases. There have been a number of suggestions over the years and it must surely depend on where you look in the Galaxy. Heiles (1994) suggested that it might be the diffuse ionized gas (WIM) that also produces the [N II] lines. Bennett *et al.* (1994), suggested that it might be the cold neutral atomic clouds (CNM). Or it could be mainly associated wth PDRs on surfaces of GMCs (Stacey *et al.* 1985, Shibai *et al.* 1991, Cubick *et al.* 2008). In regions where the [C II] line dominates the gas cooling (CNM and $n < 3 \times 10^3$ cm^{-3} GMC surfaces) the total cooling rate measured by [C II] provides the total energy input into the gas.

Another reason to sort out the [C II] emission components is for extragalactic observations. For example in a [C II] map of NGC 3521 using Herschel PACS the 10″ beam subtends a size of about 500 pc (Kennicutt *et al.* 2011). Each beam contains a mix of components and it is difficult to untangle the [C II] emission. One approach is to use the Galaxy as a template to sort out the contribution from various emitting components.

Another problem for the energy budget comes from the extragalactic [O I] 63 μm maps (e.g., NGC 3521; Kennicutt *et al.* 2011). Where there are bright H II regions the [O I] is probably radiatively heated and comes from PDRs on GMC surfaces. Emission is seen,

https://doi.org/10.1017/S1743921312016791 Published online by Cambridge University Press

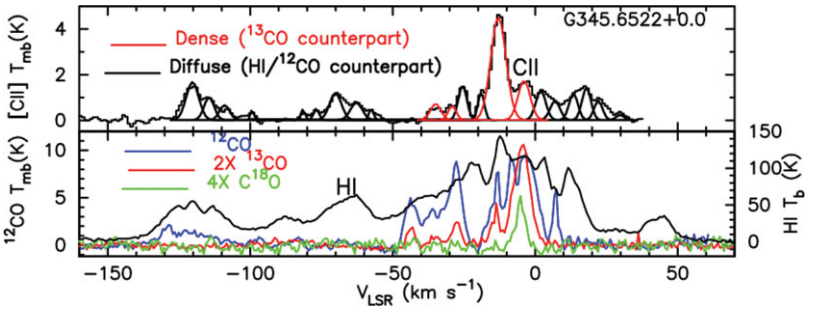

Figure 2. [C II] spectra obtained with Herschel/HIFI for the GOTC+ program at $l = 345.65°$ and $b = 0°$, along with the CO data from the Mopra telescope and H I surveys (Langer *et al.* 2010).

however, between the arms in 250 pc beams. The emission could be unresolved PDRs, but there are suggestions that the [O I] comes from diffuse gas that is mechanically heated in shocks or turbulence (Beirão *et al.* 2012). Is the wide spread [O I], radiatively or mechanically heated? One way to check is to look for [O I] emission in the Galactic diffuse ISM from Antarctica.

How would one carry out these sorts of studies? First consider a plot of thermal pressure versus density in thermal equilibrium. Along a line of constant pressure there is a stable phase of temperature $\sim$ 8000 K (the WNM) and a stable phase of temperature $\sim$ 100 K (the CNM) and in between there is a thermally unstable phase (Wolfire *et al.* 2003). The phase diagram along with heating and cooling rates can be used to estimate the cooling rate in the cold gas. The [C II] line cooling in the cold gas (CNM) ($\sim 4 \times 10^{-26}$ erg cm^{-2} s^{-1} H^{-1}) is more than a factor of 10 higher than in the warm gas (WNM). Even gas that is thermally unstable does not produce much [C II]. This means the [C II] isolates the cold clouds in emission which were previously seen only in absorption from H I absorption or FUV absorption spectroscopy.

Next one needs a large scale, velocity resolved (< 1 km s^{-1}) map in [C II] of the Galactic plane. There is a proposed Antarctic balloon project GUSSTO to do just that. GUSSTO can look along a line of sight and separate the various [C II] emitting components. The GOTC+ team has started to do this using Herschel HIFI. GOTC+ is an Open Time Herschel Key Project to observe [CII] along individual lines of sight. Figure 2 shows a GOTC+ spectrum with [C II] in the top panel, and H I and CO in the lower panel. Individual [C II] emitting components are seen. Components which show H I but no [C II] are probably the WNM. Velocities with H I and [C II] but no CO are probably CNM components. Where there is [C II], H I and CO, there is probably a molecular cloud. But note these are single lines of sight and without mapping it is hard to know if the line of sight passes a diffuse cloud, or the edge of a molecular cloud, which could be C^+ and H I, or C^+ and H_2, or if CO is observed the line-of-sight might be skimming along the edge of the molecular portion. With [C II] and resolved maps in H I and CO, it is possible to make a 3D decomposition of the [C II] emitting components and determine where the [C II] luminosity is coming from.

4. Ionised Gas

The COBE FIRAS maps show that the [N II] lines are quite bright being second to that of [C II]. If both the 205 μm and 122 μm lines can be obtained, then they can be used as indicators of the electron density. Figure 3 shows that the line ratio is sensitive to densities between $\sim$ 10 and 10^4 cm^{-3} which are high diffuse cloud densities to classic

https://doi.org/10.1017/S1743921312016791 Published online by Cambridge University Press

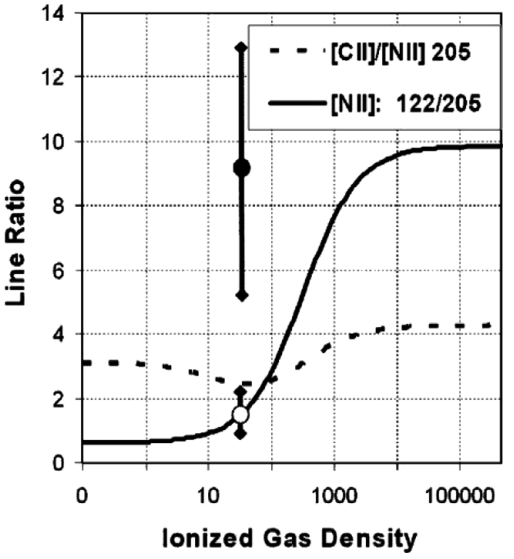

Figure 3. Ratio of [C II]/[N II] 205 μm and [N II] 122 μm/[N II] 205 μm line intensities versus density (Oberst *et al.* 2006).

H II regions. The [N II] lines can then map out the ionized gas distribution and thermal pressure in the Galaxy. Figure 3 also shows the [C II]/[N II] ratio provides an estimate of the fraction of [C II] that arises in the ionized phase. Observations can also zoom in on individual H II regions and map out the electron density and ionizing photon distribution as was done for the Carina Nebula by Oberst *et al.* (2011) using AST/RO.

5. The Dark Molecular Gas

Both observations (Smith & Madden 1997) and models (van Dishoeck & Black 1988) of cloud surfaces usually find a layer in which H turns to H_2 before C turns to CO. Using the CO alone to estimate the molecular mass misses the mass contained in the H_2 layer. This has been called the "dark molecular gas" although it is not really dark at all and emits in [C II], [C I] and dust continuum – all of which are observable from Antarctica.

Wolfire *et al.* (2010) presented PDR models of the dark molecular gas in which they 1) added a turbulent density distribution, 2) applied global GMC properties, and 3) calculated the cloud masses. These are 1D models but used the median density expected from turbulence. The median of the log-normal density distribution is given by $\langle n \rangle_{\rm med} = \bar{n} \exp(\mu)$ with $\mu = 0.5 \ln(1 + 0.25\mathcal{M}^2)$ (Padoan *et al.* 1997). The volume averaged density distribution ($\bar{n} \propto 1/r$) is the first global GMC property. The sound speed that enters in the Mach number, $\mathcal{M}$ is calculated from the PDR model output while the turbulent velocity is given by the GMC size-linewidth relation $v \propto R^{0.5}$.

Figure 4 shows the model abundances as a function of A_V into the cloud. The dashed line marked $A_V(R_{H2})$ is where gas is half molecular, and A_V(CO) is where the optical depth in CO (1-0) is equal to one. The layer between the dashed lines is the dark molecular gas (which emits in [C II], [C I] and IR continuum).

If $M(R_{\rm H_2})$ is the molecular mass within the radius where the molecular fraction is 0.5, and M(CO) is the mass within the radius of the $\tau_{\rm CO} = 1$ surface, then the dark gas fraction can be defined as $f_{\rm DG} = [M(R_{\rm H_2}) - M(R_{\rm CO})]/M(R_{\rm H_2})]$. Figure 5 shows the calculated $f_{\rm DG}$ for several GMC mass and FUV radiation fields. We find a rather constant fraction of about $\sim 30\%$. This value agrees reasonably well with the EGRET

https://doi.org/10.1017/S1743921312016791 Published online by Cambridge University Press

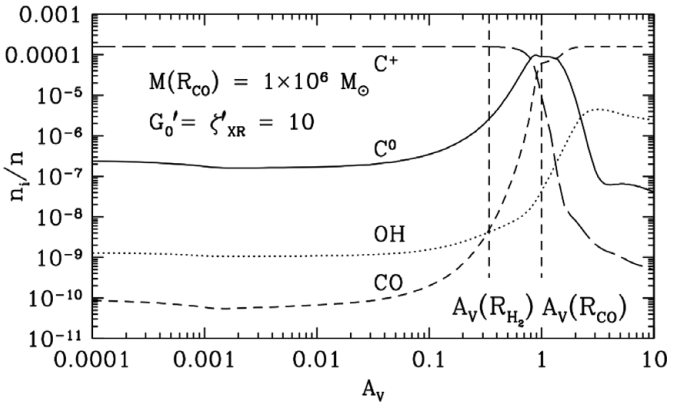

Figure 4. Abundances of C^+ (long-dashed curve), C^0 (solid curve), OH (dotted curve) and CO (short-dashed curve) as functions of optical depth into the cloud for $M = 1 \times 10^6\ M_\odot$, Galactic dust and metals, and incident radiation field $G_0' = \chi = 10$. Note that we do not include freeze out of H_2O on grain surfaces, which would affect OH abundances at $A_V > 3$ (Hollenbach *et al.* 2009).

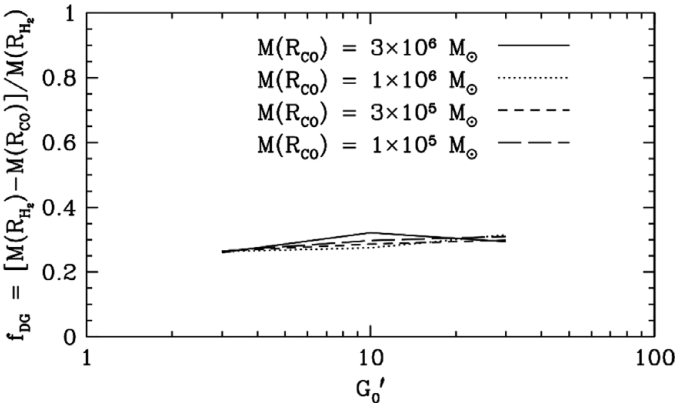

Figure 5. Dark-gas fraction $f_{\rm DG}$ versus incident radiation field normalized to the local interstellar field, $G_0' = \chi = G_0/1.7$.

gamma ray observations (Grenier *et al.* 2005), but slightly lower than the Fermi gamma ray observations (Abdo *et al.* 2010) and those based on Planck IR continuum observations (Planck Collaboration *et al.* 2011). A simple expression for the dark gas fraction is given by

$$f_{\rm DG} = 1 - \exp\left(\frac{-4.0\Delta A_V}{\bar{A}_V}\right), \tag{5.1}$$

where ΔA_V is the optical depth in the dark gas layer and $\bar{A}_V = 5.26 Z \bar{N}_{22}$ is the mean optical depth through the CO portion. Here, Z is dust abundance relative to the local Galactic conditions, and $\bar{N}_{22}$ is the column density in units of 10^{22} cm^{-2} through the CO portion. The higher $f_{\rm DG}$ values determined by Fermi and Planck may be due to lower cloud columns sampled by these surveys.

6. Terahertz Interferometry

An intriguing prospect is to conduct Terahertz Interferometry from Antarctica made possible in part due to the longer coherent times that can be achieved. One project might

https://doi.org/10.1017/S1743921312016791 Published online by Cambridge University Press

be to revisit the Herschel PACS [C II] and [O I] extragalactic maps with greater spatial resolution to separate the emitting components. The PACS observations are $\sim 10''$ and with ~ 20 times greater resolution at 11 Mpc, the GMCs will start to be resolved in [C II] emission. Another project might be to observe the protostellar outflows as modeled in van Kempen *et al.* (2010) and Visser *et al.* (2012). The rotational line emission of CO is observed to very high-J (~ 33) levels covering the mm through THz bands. The models suggest that the low-J mm lines arise in a passively heated dust envelope, the mid-J sub-mm lines arise in a PDR in the outflow walls, while the high-J THz lines arise in C-shocks. Thus the CO emitting volume and kinematics vary with wavelength and it might be possible to test the theoretical predictions.

7. Conclusions

Three short conclusions are 1) good atmospheric transmission at Antarctica allows for studies in many different sub-mm and THz lines and continua probing a wide range in ISM studies. 2) Antarctica allows for large area survey or mapping modes that are not available elsewhere. 3) THz interferometry, if possible, opens unique opportunities for science exploration from Antarctica.

Acknowledgements

M.G.W. acknowledges partial support from NASA award number NNX10AM78G "The Stratospheric Terahertz Observatory".

References

Abdo, A. A., *et al.* 2010, *ApJ*, 710, 133
Beirão, P., Armus, L., Helou, G., *et al.* 2012, *ApJ*, 751, 144
Bennett, C. L., Fixsen, D. J., Hinshaw, G., *et al.* 1994, *ApJ*, 434, 587
Cubick, M., Stutzki, J., Ossenkopf, V., Kramer, C., & Röllig, M. 2008, *A&A*, 488, 623
Gerin, M. *et al.* 2010, *A&A*, 518, L110
Gorti, U. & Hollenbach, D. 2009, *ApJ*, 690, 1539
Grenier, I. A., Casandjian, J.-M., & Terrier, R. 2005, *Science*, 307, 1292
Heiles, C. 1994, *ApJ*, 436, 720
Hollenbach, D., Kaufman, M. J., Bergin, E. A., & Melnick, G. J. 2009, *ApJ*, 690, 1497
Kennicutt, R. C., Calzetti, D., Aniano, G., *et al.* 2011, *PASP*, 123, 1347
Langer, W. D., Velusamy, T., Pineda, J. L., *et al.* 2010, *A&A*, 521, L17
Lawrence, J. S. 2004, *PASP*, 116, 482
Neufeld, D. A., Falgarone, E., Gerin, M., *et al.* 2012, *A&A*, 542, L6
Oberst, T. E., Parshley, S. C., Stacey, G. J., *et al.* 2006, *ApJL*, 652, L125
Oberst, T. E., Parshley, S. C., Nikola, T., *et al.* 2011, *Apj*, 739, 100
Padoan, P., Jones, B. J. T., & Nordlund, A. P. 1997, *ApJ*, 474, 730
Planck Collaboration, Ade, P. A. R., Aghanim, N., *et al.* 2011, *A&A*, 536, A19
Shibai, H., Okuda, H., Nakagawa, T., *et al.* 1991, *ApJ*, 374, 522
Smith, B. J. & Madden, S. C. 1997, *AJ*, 114, 138
Stacey, G. J., Viscuso, P. J., Fuller, C. E., & Kurtz, N. T. 1985, *ApJ*, 289, 803
van Dishoeck, E. F. & Black, J. H. 1988, *ApJ*, 334, 771
van Kempen, T. A., Kristensen, L. E., Herczeg, G. J., *et al.* 2010, *A&A*, 518, L121
Visser, R., Kristensen, L. E., Bruderer, S., *et al.* 2012, *A&A*, 537, A55
Wright, E. L., Mather, J. C., Bennett, C. L., *et al.* 1991, *ApJ*, 381, 200
Wolfire, M. G., Hollenbach, D., & McKee, C. F. 2010, *ApJ*, 716, 1191
Wolfire, M. G., McKee, C. F., Hollenbach, D., & Tielens, A. G. G. M. 2003, *ApJ*, 587, 278